Appl Phys B (2011) 105:715–720
DOI 10.1007/s00340-011-4795-6

Applied Physics B
Lasers and Optics

Narrow-band, tunable 2 μm optical parametric oscillator based on MgO:PPLN at degeneracy with a volume Bragg grating output coupler

P. Koch · F. Ruebel · M. Nittman · T. Bauer · J. Bartschke · J.A. L'huillier

Received: 19 April 2011 / Revised version: 12 September 2011 / Published online: 12 November 2011

Abstract A degenerate optical parametric oscillator (OPO) using an MgO:PPLN crystal and a volume Bragg grating (VBG) output coupler is presented. By changing the temperature of the VBG, the resonance of the OPO can be tuned exactly on the degeneracy point. A single-longitudinal and a multi-longitudinal mode pump scheme as well as the performance of the optical parametric oscillator on and off degeneracy are compared. It was found that the multi-longitudinal mode pump setup provides superior results with respect to spectral width and stability at degeneracy. At 2128.4 nm, a spectral width of less than 0.7 nm, an output power of 1.7 W with a slope efficiency of 31.8%, and low power fluctuation of 0.3% were achieved.

1 Introduction

Coherent radiation in the mid-infrared is of interest for many applications such as spectroscopy, trace gas analysis, remote sensing, medicine and homeland security. However tunable, pulsed solid-state laser sources beyond 4 μm are difficult to obtain. Because of the high transparency of $ZnGeP_2$ (ZGP) in this spectral region and its high nonlinear coefficient, ZGP based OPOs are an interesting approach for the generation of MIR radiation, but require pump wavelengths longer than 2 μm. For direct pumping, holmium-lasers are suitable, which are typically pumped with thulium bulk [1] or fiber lasers [2]. An interesting alternative source for the 2 μm pump beam is an OPO pumped by a well developed and reliable 1.06 μm neodymium-laser. In such tandem OPO setups [3–8], the first conversion stage should provide a high spectral power density to achieve efficient conversion in the second stage. Using a type-II OPO in the first conversion stage provides a narrow spectrum even close to degeneracy, but the signal and idler radiation is orthogonally polarized. So only one beam can be used for pumping a second conversion stage [3–5]. In type-I and quasi-phase-matched (QPM) OPOs, the polarization of the signal and idler radiation is parallel and both can be used for a further conversion stage. However, free-running QPM OPOs generate very broadband spectra around degeneracy. Possible mechanisms to narrow the linewidth are the usage of intracavity etalons [9] and gratings [10] and injection seeding [11]. But these concepts cause either high losses or require complex setups. A simple and efficient method to narrow the spectrum of an OPO is employing a volume Bragg grating (VBG) as output coupler, which has first been demonstrated in the near-infrared by Jacobsson et al. [12]. Henriksson et al. transferred this concept to the 2 μm region and demonstrated subsequently several setups operating at 2008 nm [6, 13] and 2122 nm [8] and very close to degeneracy at 2127.8 nm [7] and 2128 nm [8]. Saikawa et al. reported on two high-energy setups at degeneracy with an FWHM of less than 1.4 nm [14] and 2 nm [15], respectively. Thilmann et al. demonstrated a 532 nm pumped OPO which is tunable and narrow-band around degeneracy via a transversely chirped Bragg grating [16]. Blau et al. demonstrated the tuning of the resonance of an OPO at 2.5 μm by changing the temperature of a VBG [17]. Smith et al. investigated degenerate type I OPOs in a stabilized ring cavity pumped by a single longitudinal mode laser [18]. Thereby the stabilization

P. Koch (✉) · F. Ruebel · J.A. L'huillier
Photonik-Zentrum Kaiserslautern e.V., Kohlenhofstrasse 10,
67663 Kaiserslautern, Germany
e-mail: peter.koch@pzkl.de
Fax: +49-(0)-631-41557510

M. Nittman · T. Bauer · J. Bartschke
Xiton Photonics GmbH, Kohlenhofstrasse 10,
67663 Kaiserslautern, Germany

of the cavity length is a critical aspect in order to achieve stable operation at degeneracy. Therefore, Henriksson et al. preferred an oscillating wavelength not exactly at the degeneracy point to ensure stable operation [7]. In our work, we focused on realizing a narrow-band 2 µm PPLN-OPO in a high repetition rate setup which can be tuned exactly on the degeneracy point (2128.4 nm). Such a setup should provide a high spectral power density for a second conversion stage. By changing the temperature of the volume Bragg grating, the wavelength can be tuned. By using a multi longitudinal mode laser, the phase fluctuations of the signal and idler radiation should be averaged across the longitudinal pump modes and therefore stable operation exactly at the degeneracy point should be possible even with an unstabilized linear cavity. In order to investigate this behavior in detail, we used two different pump schemes: a single-longitudinal and a multi-longitudinal mode laser setup. Both configurations are compared with respect to wavelength tunability and spectral properties and stability off and on degeneracy.

2 Experimental setup

The optical parametric oscillator consisted of a linear unstabilized cavity with a length of 60 mm. Two different pumping schemes were used: a single-longitudinal (SL) and a multi-longitudinal (ML) mode laser setup.

The pump laser for the single-longitudinal mode pump setup was a Q-switched Nd:YVO_4-laser which provided 11.2 ns pulses at 10 kHz repetition rate with 4.8 W maximum output power. The laser had a spectral bandwidth of 34.5 MHz at a wavelength of 1064.07 nm with an excellent beam quality ($M^2 < 1.1$). The pump laser for the multi-longitudinal mode setup was a Q-switched Nd:YVO_4-laser (Xiton Photonics XVL-AMP-Q) which provided a spectral bandwidth of 19 GHz (approx. 25 modes) at a wavelength of 1064.2 nm. The mode-spacing of the longitudinal modes was approx. 742 MHz. The pulse length was 12 ns at a repetition rate of 15 kHz with a maximum output power of 11.3 W in a diffraction limited beam ($M^2 < 1.1$). The nonlinear crystal for the OPO, which was pumped by the single-longitudinal mode laser (SL setup), was a homemade periodically poled Mg-doped $LiNbO_3$-crystal with a poling period of 31.8 µm. In order to ensure phasematching and hence maximum gain exactly at degeneracy, the temperature of the crystal was stabilized at 149.8°C. The crystal had a length of 20 mm and was AR-coated for 1064 nm and in the range from 2000 to 2300 nm. Unfortunately, this crystal was damaged after the measurements with the SL setup. Therefore, we used another homemade crystal for the OPO, which was pumped by the multi-longitudinal mode laser (ML setup). The crystal had a poling period of 31.9 µm and its temperature was stabilized at 132.5°C for maximum gain at degeneracy. Both crystals had the same length and the same coating. Hence the operating conditions of both crystals were well comparable. In the SL setup, the pump beam was focused to a 162×144 µm^2 waist in the crystal. The ML setup used a similar focus (151×146 µm^2) to ensure comparability of both setups. For the ML setup, a maximum pump power of 8 W was used in order to avoid damage of the crystal by exceeding the damage threshold, by green induced infrared absorption (GRIIRA) [19] and by photorefractive effects [20]. In order to avoid residual broadband feedback at the facets, both crystals were slightly tilted (<2°).

The incident pump powers on the crystals were controlled with a $\lambda/2$-plate and a thin-film-polarizer. The input coupler of the OPO was highly transmissive at 1064 nm and highly reflective from 2060 to 2300 nm. A volume Bragg grating (ONDAX, Inc.) was used as an output coupler for both setups due to its narrow-band (FWHM 0.5 nm) reflectivity of approximately 55% centered at 2128 nm. By controlling the temperature of the VBG, the resonance of the OPO could be tuned around degeneracy. Exactly at the degeneracy point of the ML setup (2128.4 nm), the mode-spacing of the OPO modes was 1.77 GHz at the maximum reflectivity and decreased to 1.75 GHz at the first zero of the VBG's reflectivity. The calculations thereby considered the group delay in the VBG as demonstrated by Henriksson et al. [21]. Hence the operation point of the OPO was aside any cavity length resonances which have been reported by Henriksson et al. for a singly resonant OPO [22] and by Arisholm et al. for a doubly resonant OPO [4].

3 Results and discussion

The behavior of the SL-setup and the ML-setup around degeneracy is investigated with respect to tunability, output energy, stability, and spectrum.

3.1 Tunability

The output power of the OPO in dependence of the oscillating wavelength is shown in Fig. 1. Wavelength tuning was achieved by tuning the temperature of the VBG from 30 to 90°C. The tuning rate was approximately 0.0244 nm/°C. The degeneracy point for the SL-setup (red line in Fig. 1(a)) differs from the one for the ML-setup (blue line in Fig. 1(b)) due to the slightly different wavelengths of the pump lasers (see Sect. 2). Complete double resonance of the OPO is reached at the degeneracy point (points P1 and P2 in Fig. 1). In the shaded areas in Fig. 1, the signal and idler spectra overlap, and thus the OPO is partially doubly resonant. Outside of this shaded area in Fig. 1, the OPO is single resonant on the signal wave or the idler wave, respectively. The decrease of the output power at degeneracy is a result of the lower output coupling of the OPO for doubly resonant operation. Considering only the peak reflectivity of

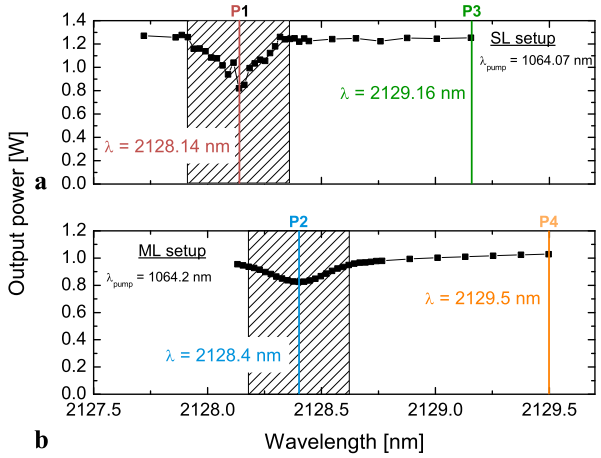

Fig. 1 Tuning of the OPO's resonance by increasing the temperature of the volume Bragg grating from 30 to 90°C for the SL setup (**a**) and the ML setup (**b**). The *shaded areas* mark approximately the range where the OPO is partially or completely doubly resonant. The temperature of the VBG increases from *left* to *right*. For further details see text

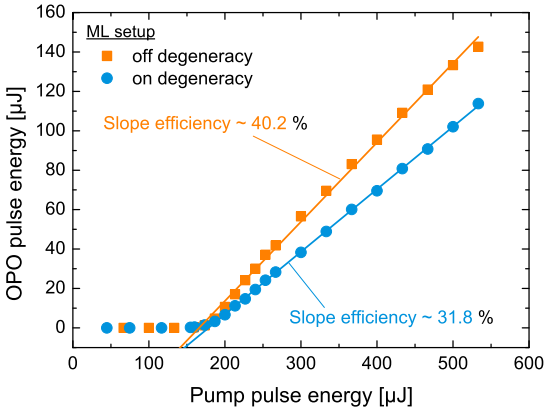

Fig. 2 Output energy of the ML setup for the operating regimes on and off degeneracy

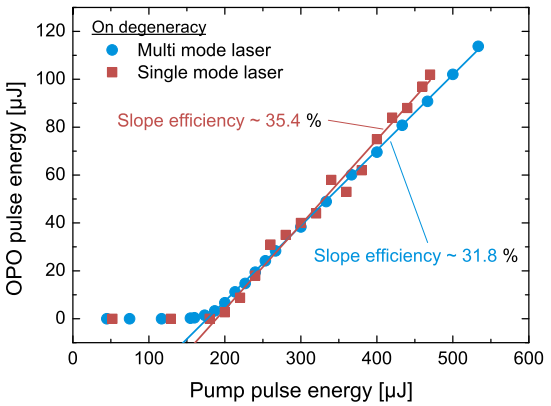

Fig. 3 Output energy at degeneracy for the SL setup and the ML setup

the VBG, as an approximation, the maximum reflectivity of 55% results in an output coupling of 45% on the identical signal and idler wave. The actual output coupling is higher because the spectrum of the OPO is wide enough (see Sect. 3.4) so that the reflectivity of the VBG varies inside the spectrum. For singly resonant operation, the resonant wave has an output coupling of 45% and the nonresonant wave an output coupling of 100%, leading to an overall output coupling of 72.5% (by neglecting the difference in photon energy). For a detailed investigation, a Rigrod analysis is necessary, which is beyond the scope of this work. Another effect that could decrease the efficiency at degeneracy is second harmonic generation (SHG) of the signal and idler, which has been simulated by Henriksson et al. [8]. The phase mismatch for SHG of the signal and idler near and on degeneracy is low. Therefore, SHG is an additional backconversion process which adds to the backconversion losses through sum frequency mixing of the signal and idler. The tuning characteristics of the SL-setup and the ML-setup are very similar. The volume Bragg grating allows both setups to be tuned exactly on the degeneracy point. In the following sections, the SL and the ML setup are compared with respect to pulse energy, efficiency and spectrum for the on degeneracy operating regime (points P1 and P2 in Fig. 1) and the off degeneracy operating regime (points P3 and P4 in Fig. 1).

3.2 Pulse energy

In Fig. 2, the pulse energy of the ML-setup on and off degeneracy (points P2 and P4 in Fig. 1) is shown in dependence of the pump energy. The threshold for both operating regimes is about 180 µJ. When operating off degeneracy a maximum output energy of 143 µJ was achieved, which corresponds to a conversion efficiency of 26.8%. The slope efficiency is 40.2%. The OPO at degeneracy has a maximum output energy of 114 µJ (approximately 1.7 W average power) with a slope efficiency of 31.8% and a conversion efficiency of 21.3%. The configuration operating at degeneracy provides lower performance values because of the lower output coupling in the doubly resonant operation. A similar behavior can be observed with the SL-setup. The output energy in dependence of the pump energy at degeneracy for the SL-setup and the ML-setup (points P1 and P2 in Fig. 1) is compared in Fig. 3. The SL setup at degeneracy provides a threshold of 190 µJ and a slope efficiency of 35.4%. The maximum output energy of 102 µJ corresponds to a conversion efficiency of 21.7%. So the performance values at degeneracy are very similar for the SL and the ML setup. This is different from the results obtain by Smith et al. [18] where the threshold for the ML pump is by a factor of 3 to 4 higher. We believe this is because Smith et al. stabilized the ring cavity, and therefore achieved optimum gain in the SL setup, which was not the case in our unstabilized linear cavity.

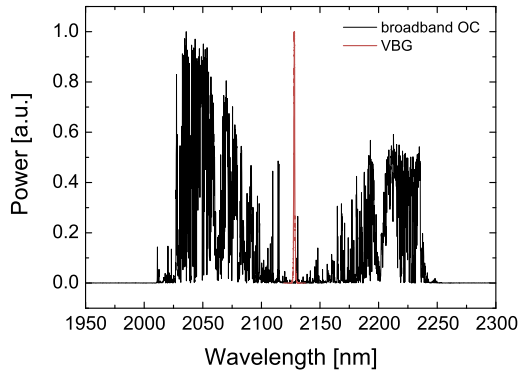

Fig. 4 Spectral splitting of the OPO with a broadband output coupler (OC) at degeneracy pumped by the SL laser (*black curve*). The VBG narrows the spectrum by a factor of more than 200 (*red curve*)

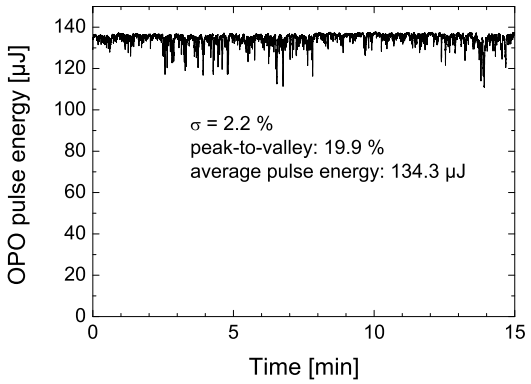

Fig. 5 Stability of the OPO's pulse energy at degeneracy by using a broadband output coupler. The OPO is pumped by the single-longitudinal mode laser and is operated 2.3 times above threshold

3.3 Stability for operation on the degeneracy point

With respect to tunability, threshold and efficiency the SL and the ML-setup at degeneracy are comparable. Therefore, it is interesting to investigate the stability of both setups at the degeneracy point (points P1 and P2 in Fig. 1), since this is a critical aspect if the OPO is used as a pump source for a further conversion stage. Smith et al. [18] investigated theoretically and experimentally the fact that in a doubly resonant OPO (DRO) the round-trip phase of the signal is a critical aspect. For optimum energy transfer from the pump to the signal and idler, the following phase relationship has to be fulfilled [23]:

$$\phi_p = \phi_s + \phi_i + \frac{\pi}{2}. \tag{1}$$

At degeneracy the signal and idler are indistinguishable, and therefore (1) becomes

$$\phi_p = 2\phi_{s,i} + \frac{\pi}{2}. \tag{2}$$

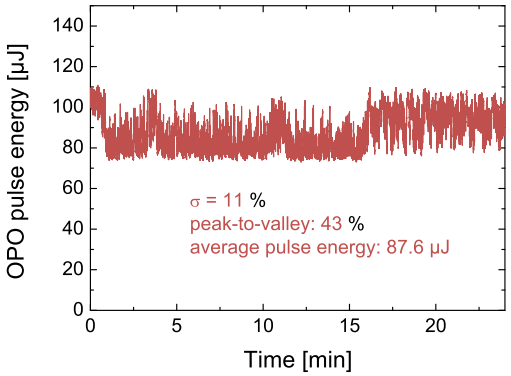

Fig. 6 Stability of the OPO's pulse energy at degeneracy by using the VBG for output coupling. The OPO is pumped by the single-longitudinal mode laser and is operated 2.5 times above threshold

In a singly resonant OPO (SRO), the nonresonant wave can adapt freely to the accumulated round-trip-phase of the resonant phase so that (1) is fulfilled and the signal and idler experience optimum gain. In a DRO, this is not the case and the cavity length has to be stabilized in order to have maximum gain. Smith et al. studied numerically and experimentally the fact that in a DRO at degeneracy the accumulated round-trip phase can be compensated by a splitting of the spectrum or a distortion of the beam. The spectral splitting is on the order of magnitude of the acceptance bandwidth [18].

Using the OPO with a broadband output coupler and the SL pump laser, we also observed spectral splitting which is shown in Fig. 4 (black curve). The broadband output coupler has a reflectivity of approximately 3%. The spectrum shows severe modulations which are caused by mode hopping during the measurement. In Fig. 5, the stability of the broadband setup is shown. The OPO has poor stability with fluctuations of 2.2% RMS and 19.9% peak-to-valley. Small variations of the cavity length through vibrations or temperature fluctuations change the round-trip phase of the signal and therefore have a huge impact on the conversion efficiency, which has already been shown by Smith et al. [18]. Smith et al. concluded that the cavity length has to be stabilized on 1% of the signal wavelength.

Figure 6 shows the stability of the narrow-band SL setup with the VBG exactly at degeneracy. The setup suffers under severe pulse energy fluctuations of 11% RMS and 43% peak-to-valley. Because of the narrow-band reflectivity of the VBG, a splitting of the spectrum, like in the broadband setup, is not possible (Fig. 4, red curve), and therefore the phase errors of the signal cannot be compensated. Hence the stability of the narrow-band OPO pumped by the SL laser is worse compared to the broadband OPO, which is pumped by the SL laser as well.

In contrast to that, the narrow-band OPO, which is pumped by the ML laser and operated exactly at degeneracy shows a more stable behavior. The pulse energy has

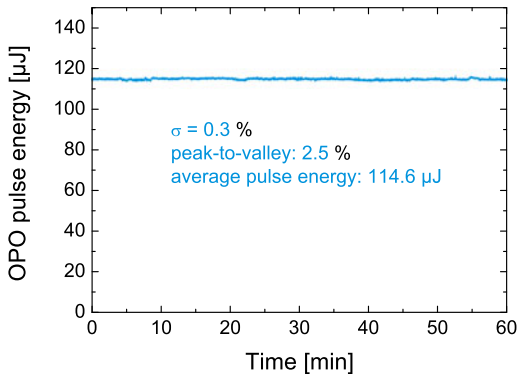

Fig. 7 Stability of the OPO's pulse energy at degeneracy by using the VBG for output coupling. The OPO is pumped by the multi-longitudinal mode laser and is operated 3 times above threshold

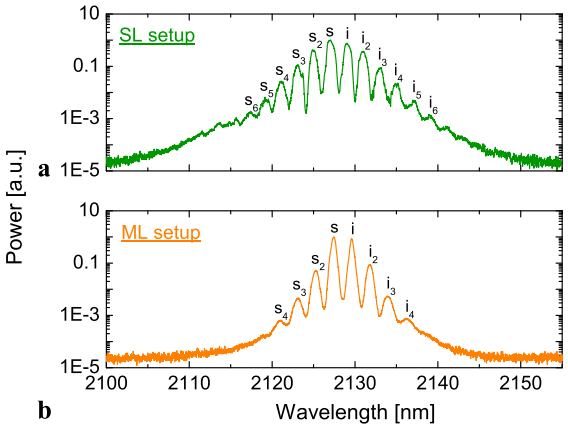

Fig. 8 Spectra for the off degeneracy operating regime. Comparison between the SL-setup and the ML-setup. For further details see text

low fluctuations with 0.3% RMS and 2.5% peak-to-valley (see Fig. 7). We believe the increased stability of the ML setup is the result of an averaging effect of the longitudinal pump modes. The pump phase ϕ_p from (2) is constant in the SL setup during the pump pulse and between consecutive pulses. In the ML setup, this is not the case. Because of mode-beating of the longitudinal modes, the phase is not constant during the pulse and changes randomly. Hence the phase relationship (2) is not exactly defined, and the phase errors are averaged. This leads to an increased stability of the ML setup compared to the SL setup, and therefore the ML setup is better suited as a pump source for a further conversion stage.

3.4 Spectra of the OPO around degeneracy

In Fig. 8, the spectra for the off-degeneracy operating regime (points P3 and P4 in Fig. 1) are shown for the SL setup and the ML setup. Apart from the signal and idler peak, also adjacent maxima in the spectra can be observed. These peaks are caused by four wave mixing (FWM), which has also

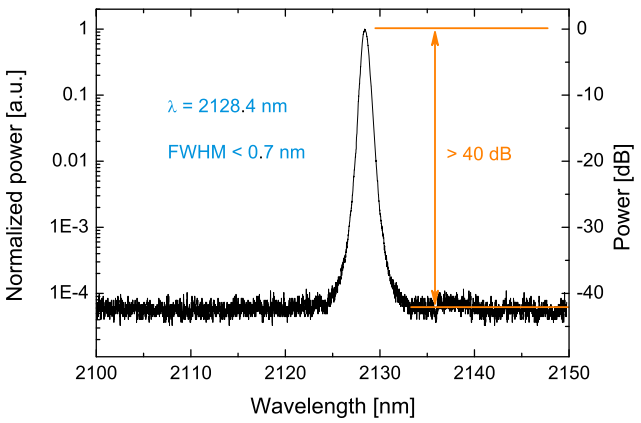

Fig. 9 Spectrum of the ML setup at degeneracy

been observed by Thilmann et al. [16]. Close to degeneracy, the phase mismatch for SHG of the signal and idler radiation is very small. This leads to additional wavelengths close to the pump wavelength which can interact with the signal and idler via difference frequency generation (DFG). This secondary signal ($\omega_{s2} = 2\omega_s - \omega_i$) and idler ($\omega_{i2} = 2\omega_i - \omega_s$) peaks are within the gain bandwidth of the OPO and are further amplified to a detectable power level. In Fig. 8, there are also higher order FWM peaks visible, caused subsequently by SHG of the FWM peaks. Thereby, the spectrum of the SL setup contains more additional peaks than the one of the ML setup. We believe this is the case because in the SL setup the gain cannot be completely depleted by the resonating idler wave due to the phase errors in this unstabilized linear cavity (see Sect. 3.3). Therefore, the gain for parasitic effects is much higher than in the ML setup. Hence more higher order FWM peaks occur in the SL setup. Furthermore, the main signal and idler peaks of the ML setup are narrower than in the SL setup. This might be caused by FWM within the main peak. Since this parasitic effect is more efficient in the SL setup, its main peak is also broader. The FWHM of the idler is 0.42 nm and 0.85 nm for the ML setup and the SL setup, respectively.

In Fig. 9, the spectrum at degeneracy is shown for the ML setup. The OPO oscillates exactly at the degeneracy point ($\lambda = 2128.4$ nm) without any adjacent maxima and a spectral bandwidth of less than 0.7 nm (FWHM). The suppression of the broadband background is thereby better than 40 dB. The spectral bandwidth of the SL setup on degeneracy is 0.9 nm, and therefore larger than in the ML setup, which we attribute to FWM within the main peak.

3.5 Beam quality of the OPO around degeneracy

The beam profile of the OPO has an almost Gaussian shape with a minor ellipticity and asymmetry. The M^2 measurements for both setups around degeneracy result in values between 2 and 3.2. In Fig. 10, the beam profile and the

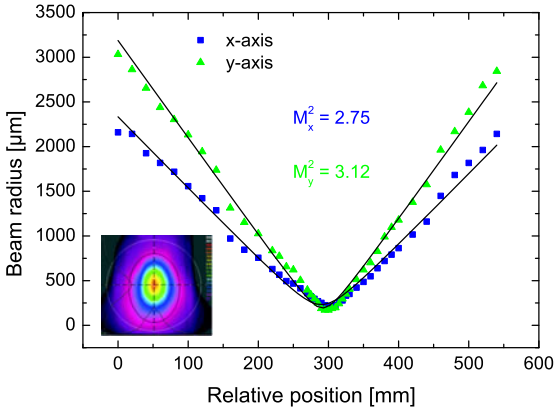

Fig. 10 M^2 measurement and beam profile at degeneracy for the ML-setup

M^2 measurement is shown for the ML-setup at degeneracy (point P2 in Fig. 1). Exactly at the degeneracy point, an M^2 of 2.75 in the x-direction and 3.12 in the y-direction was achieved.

4 Conclusion

We have demonstrated a 2 µm optical parametric oscillator with a volume Bragg grating output coupler which is tunable around the degeneracy point. The tunability was realized by changing the temperature of the VBG. By tuning the resonance of the OPO, we realized oscillation exactly at the degeneracy point. We used a single-longitudinal mode and a multi-longitudinal mode laser pump setup in order to investigate the influence of the spectral properties of the pump laser on the performance of the OPO with an unstabilized linear cavity. Due to an averaging effect of the phase fluctuations of the signal and idler radiation across the longitudinal pump modes, the multi-longitudinal mode laser configuration features an increased stability and spectral quality compared to the single-longitudinal mode laser setup. Therefore, the ML-setup is considerably better suited as a pump source for further conversion stages.

Exactly at the degeneracy point, the ML configuration provides a maximum output power of 1.7 W which corresponds to a pulse energy of 114 µJ and a conversion efficiency of 21.3%. The slope efficiency is 31.8%, and the setup provides low power fluctuations of 0.3% RMS and good beam quality. The spectral width at 2128.4 nm is less than 0.7 nm. Therefore, the OPO has excellent properties and is well suited as a pump source for a second conversion stage in a ZGP tandem OPO setup.

References

1. P.A. Budni, L.A. Pomeranz, M.L. Lemons, C.A. Miller, J.R. Mosto, E.P. Chicklis, J. Opt. Soc. Am. B **17**, 723 (2000)
2. E. Lippert, S. Nicolas, G. Arisholm, K. Stenersen, G. Rustad, Appl. Opt. **45**, 3839 (2006)
3. P.B. Phua, K.S. Lai, R.F. Wu, T.C. Chong, Opt. Lett. **23**, 1262 (1998)
4. G. Arisholm, E. Lippert, G. Rustad, K. Stenersen, Opt. Lett. **25**, 1654 (2000)
5. K. Miyamoto, H. Ito, Opt. Lett. **32**, 274 (2007)
6. M. Henriksson, M. Tiihonen, V. Pasiskevicius, F. Laurell, Opt. Lett. **31**, 1878 (2006)
7. M. Henriksson, M. Tiihonen, V. Pasiskevicius, F. Laurell, Appl. Phys. B **88**, 37 (2007)
8. M. Henriksson, L. Sjöqvist, G. Strömqvist, V. Pasiskevicius, F. Laurell, Proc. SPIE **7115**, 71150O (2008)
9. G. Robertson, A. Henderson, M.H. Dunn, Appl. Phys. Lett. **62**, 123 (1993)
10. W.R. Bosenberg, D.R. Guyer, Appl. Phys. Lett. **61**, 387 (1992)
11. J.E. Bjorkholm, H.G. Danielmeyer, Appl. Phys. Lett. **15**, 171 (1969)
12. B. Jacobsson, M. Tiihonen, V. Pasiskevicius, F. Laurell, Opt. Lett. **30**, 2281 (2005)
13. M. Henriksson, L. Sjöqvist, V. Pasiskevicius, F. Laurell, Appl. Phys. B **86**, 497 (2007)
14. J. Saikawa, M. Fujii, H. Ishizuki, T. Taira, Opt. Lett. **32**, 2996 (2007)
15. J. Saikawa, M. Miyazaki, M. Fujii, H. Ishizuki, T. Taira, Opt. Lett. **33**, 1699 (2008)
16. N. Thilmann, B. Jacobsson, V. Pasiskevicius, F. Laurell, E. Rotari, V. Smirnov, L. Glebov, in *Conference on Lasers and Electro-Optics/International Quantum Electronics Conference, OSA Technical Digest (CD)* (Optical Society of America, Washington, 2009), paper CWC1
17. P. Blau, S. Pearl, S. Fastig, R. Lavi, IEEE J. Quantum Electron. **44**, 867 (2008)
18. A.V. Smith, D.J. Armstrong, M.C. Phillips, R.J. Gehr, G. Arisholm, J. Opt. Soc. Am. B **20**, 2319 (2003)
19. Y. Furukawa, K. Kitamura, A. Alexandrovski, R.K. Route, M.M. Fejer, G. Foulon, Appl. Phys. Lett. **78**, 1970 (2001)
20. A. Ashkin, G.D. Boyd, J.M. Dziedzic, R.G. Smith, A.A. Ballman, J.J. Levinstein, K. Nassau, Appl. Phys. Lett. **9**, 72 (1966)
21. M. Henriksson, L. Sjöqvist, V. Pasiskevicius, F. Laurell, Opt. Express **17**, 17582 (2009)
22. M. Henriksson, L. Sjöqvist, V. Pasiskevicius, F. Laurell, Opt. Express **18**, 10742 (2010)
23. J.A. Armstrong, N. Bloembergen, J. Ducuing, P.S. Pershan, Phys. Rev. **127**, 1918 (1962)